



## Soil deformation analysis through fluid-dynamic modelling and DInSAR measurements: a focus on groundwater withdrawal in the Ravenna area (Italy)

I. ANTONCECCHI<sup>1,2</sup>, F. CICCONE<sup>1,3</sup>, G. ROSSI<sup>1</sup>, G. AGATE<sup>2</sup>, F. COLUCCI<sup>2</sup>,  
F. MOIA<sup>2</sup>, M. MANZO<sup>4</sup>, R. LANARI<sup>4</sup>, M. BONANO<sup>4</sup>, C. DE LUCA<sup>4</sup>,  
L. CALABRES<sup>5</sup>, L. PERINI<sup>5</sup>, P. SEVERI<sup>5</sup>, G. PEZZO<sup>6</sup>, P. MACINI<sup>7</sup>,  
C. BENETATOS<sup>8</sup>, V. ROCCA<sup>8</sup>, E. CARMINATI<sup>9</sup>, A. BILLI<sup>10</sup> AND L. PETRACCHINI<sup>10</sup>

<sup>1</sup> Ministero dello Sviluppo Economico, Direzione Generale per le Infrastrutture e la Sicurezza dei Sistemi Energetici e Geominerari (ex DGS-UNMIG), Roma, Italy

<sup>2</sup> Ricerca Sistema Energetico, RSE S.p.A., Milano, Italy

<sup>3</sup> Consiglio Nazionale delle Ricerche, CNR-ISMAR, Bologna, Italy

<sup>4</sup> Consiglio Nazionale delle Ricerche, CNR-IREA, Napoli, Italy

<sup>5</sup> Regione Emilia-Romagna, Bologna, Italy

<sup>6</sup> Istituto Nazionale di Geofisica e Vulcanologia, Osservatorio Nazionale Terremoti, Roma, Italy

<sup>7</sup> Dipartimento di Ingegneria Civile, Chimica, Ambientale e dei Materiali, DICAM, Università di Bologna, Italy

<sup>8</sup> Dipartimento di Ingegneria dell'Ambiente, del Territorio e delle Infrastrutture, Politecnico di Torino, Italy

<sup>9</sup> Dipartimento di Scienze della Terra, Università La Sapienza, Roma, Italy

<sup>10</sup> Consiglio Nazionale delle Ricerche, CNR-IGAG, Roma, Italy

(Received: 22 May 2020; accepted: 15 December 2020)

**ABSTRACT** This study aims at assessing the deformation processes affecting an area NW of the city of Ravenna (northern Italy), caused by groundwater withdrawal activities. *In situ* data, geologic and structural maps, piezometric measurements, underground water withdrawal volumes, and satellite C-band SAR data were used to jointly exploit two different techniques: 1) fluid-dynamic and geomechanical modelling (by RSE S.p.A), and 2) Differential Synthetic Aperture Radar Interferometry (DInSAR) analysis (by CNR - IREA). The results of the comparative analysis presented in this work brought new evidence about the contribution of groundwater withdrawal to the total subsidence affecting the area during the 2000-2017 time interval. In particular, they show an increase of the subsidence from year 2000 to 2010 and a decrease from year 2010 to 2017. These results are generally in line with groundwater withdrawal data that report a reduction of the extracted water volumes during the considered temporal interval. Meantime, they show a delay effect in the subsidence process, partially recovered during the 2010-2017 thanks to a stabilisation of the extracted groundwater volumes. The presented results shade new light on the groundwater withdrawal contribution to the subsidence of the analysed zone, although further investigations are foreseen to better clarify the ongoing scenario.

**Key words:** Soil deformation, DInSAR analysis, numerical simulation, fluid-dynamic modelling, groundwater withdrawal.

## 1. Introduction

Subsidence and local uplift are processes frequently observed in the Po Plain area (northern Italy) and in the Adriatic off-shore have been the focus of numerous investigations (e.g. Gambolati *et al.*, 1991; Teatini *et al.*, 1998; Gambolati and Teatini, 2015; Benetatos *et al.*, 2017, 2020; Coti *et al.*, 2018). Subsidence and local uplift in the Po Plain area can be attributed to several climate driven factors like floods, Messinian salinity crisis, regional uplift, and loss of accommodation space in Po basin (Carminati and Martinelli, 2002; Scardia *et al.*, 2012; Amadori *et al.*, 2018). Subsidence in the Adriatic Sea coastline, in particular, can be ascribed to different natural and anthropogenic factors locally impacting in different manner: tectonic movements, glacial isostatic adjustment, natural sediments compaction, reclaimed peatland oxidation, groundwater withdrawal, oil and gas extraction, and storage (Bertoni *et al.*, 1995; Carminati and Martinelli, 2002; Carminati *et al.*, 2003b; Teatini *et al.*, 2005; Fiaschi *et al.*, 2017). These processes are particularly marked along the coastline of the Emilia-Romagna region, and have been investigated through several studies and technical reports (Gambolati, 1998; Gambolati *et al.*, 1999; Carminati *et al.*, 2003a; ENI and ARPAE, 2003; Regione Emilia-Romagna and ARPAE, 2007, 2008, 2010, 2018; Calabrese *et al.*, 2021; Severi, 2021). In particular, the area located between Comacchio and Ravenna city (Fig. 1), extending for about  $12.5 \times 12.5$  km<sup>2</sup> in the Emilia-Romagna region onshore, is significantly affected by subsidence related to several factors, such as oil and gas extraction and storage (<https://unmig.mise.gov.it/index.php/it/>) and groundwater withdrawal for several uses and functions, e.g. civil, industrial, irrigation, livestock, etc. (Bissoli *et al.*, 2010; Cenni *et al.*, 2013).



Fig. 1 - The blue polygon represents the study area in the Ravenna onshore.

According to the Regione Emilia-Romagna and ARPAE (2007) report, which investigates subsidence affecting the whole region by exploiting Differential Synthetic Aperture Radar (DInSAR) technique and satellite SAR data acquired during the 1992-2000 and 2002-2006 time intervals, the ground deformations in the Ravenna area are characterised by a subsidence rates of -15 mm/yr for the 1992-2000 period [when the piezometric level was about -10 m on sea level (Regione Emilia-Romagna and ARPAE, 2008) report], and of -10 mm/yr for the 2002-2006 period [when the piezometric level was about -5 m on sea level (Regione Emilia-Romagna and ARPAE, 2008) report]. These results were computed by applying the DInSAR technique known as Permanent Scatterers (PSs) to SAR data (Ferretti *et al.*, 2001) acquired from: ERS-1/2 sensors along descending orbits within the 1992-2000 time interval, ENVISAT sensor along ascending and descending orbits during the 2002-2006 period, and RADARSAT-1 sensor along ascending orbits for the 2003-2005 time period. Moreover, these DInSAR analyses were referred to pixels located in the area north (for the ERS/ENVISAT analyses) and west (for the RADARSAT analysis) of the city of Reggio Emilia (Italy).

In addition, the Regione Emilia-Romagna and ARPAE (2018) report shows the results of a subsequent interferometric analysis performed by exploiting SAR data (RADARSAT-1/2 and Cosmo-SkyMed) acquired from ascending orbits during the 2011-2016 time interval and processed via the PS technique that reveals a subsidence rate of about -5 mm/yr.

Overall, these values suggest decreasing subsidence rates and uprising piezometric level due to the diminishing of groundwater withdrawal in 1992-2016 time interval. However, on the preliminary results of the Regione Emilia-Romagna and ARPAE (2008) report it is specified that:

- in several areas a strong spatial and temporal correlation between groundwater withdrawal activity, piezometric level and subsidence is noticeable;
- in localised areas along the coastline and sometimes inland subsidence appears to be not totally correlated to groundwater withdrawal;
- in some areas the data available through piezometric measurements and well groundwater withdrawal are not sufficient to study the local subsidence, as for our study area.

In addition, the Regione Emilia-Romagna and ARPAE (2010) report revealed that the contribution of groundwater extraction to total subsidence spatially ranges between 10% at Dosso degli Angeli, located NE of the study area (Fig. 1), and 30% at Fiumi Uniti, SE of the study area (Fig. 1).

In order to investigate the impact and evaluate the amount of groundwater movements due to groundwater withdrawal and its contribution to the total subsidence in the study area, *in situ* data, such as geologic and structural maps, piezometric measurements, underground water withdrawal volumes (provided by Emilia-Romagna Region), and satellite C-band SAR data were used to integrate two different methods: a) numerical modelling to evaluate the contribution of groundwater withdrawal to ground deformation; b) satellite radar interferometry to detect and estimate the total vertical displacements in the study area. Regarding the first method, based on the availability of water withdrawal time series (see sections 3.1 and 3.2), a 3D fluid-dynamic and geomechanical modelling was carried out for the years 1975, 1990, 2000, 2010, and 2017. DInSAR analysis was performed by exploiting SAR data, acquired from ERS/ENVISAT and Sentinel-1 sensors, available for the 1995-2010 and 2015-2018 time intervals (see section 3.3), respectively. The results of the performed joint analysis allowed us to constrain the subsidence affecting the study area during these periods and to assess the contribution of groundwater withdrawal to the total vertical displacement, particularly relevant for the years 2000, 2010, and 2017.

## 2. Geological framework

The study area lays in onshore Ravenna over the south-eastern portion of the Po Plain. The Po Plain is the foreland basin of both Alps and Apennines (Doglioni, 1993). The subsidence in this area is likely to be heavily influenced by the tectonic and geodynamic processes responsible for the formation of the two mountain belts (Carminati *et al.*, 2005). These two mountain belts developed on top of two subduction zones (Carminati *et al.*, 2003a). The Alps are related to the southward dipping subduction of the European plate beneath the Adriatic plate, whereas the Apennines are generated by the westward/SW-ward dipping subduction of the Adriatic plate under the Tyrrhenian lithosphere (Doglioni, 1993; Carminati *et al.*, 1998).

The River Po sedimentary basin, which encompasses an area about 38,000 km<sup>2</sup> in size, is rapidly subsiding and filled by sediments of Alpine and Apenninic origin (Carminati *et al.*, 2003a). Tectonic structures (mainly thrust faults and related folds) are buried under ca. 2000 m of Quaternary sediments deposited in continental to marine environments (Amorosi *et al.*, 1999; Carminati *et al.*, 2003a, 2003b; Ghielmi *et al.*, 2010). Geodynamics and climatological changes (Vittori and Ventura, 1995) are the main drivers of sedimentation, which has filled the basin with alternate layers of sand and clay (Carminati *et al.*, 2003b). Pre-Quaternary rocks are characterised by a complex structure of folds and thrust faults that developed parallel to the main Apennine tectonic structures. These structures provided traps for the accumulation of natural gas and oil (Gambolati *et al.*, 1991).

A multi-layer aquifer system developed in the first ca. 500 m of sediments accumulated since the Pleistocene (Di Dio, 1998). This system consists of a sequence of stratified deposits laid down during the Quaternary and the upper Pliocene in different environments, from continental, lagoonal, and deltaic in the upper zone to littoral and marine in the lower one (Gambolati *et al.*, 1991). The dynamics of Late Quaternary (last 20,000 years) sedimentation in the south-eastern Po Plain has been directly controlled by sea level changes induced both by tectonics and deglaciation (Amorosi *et al.*, 1999).

Quaternary sediments of the Emilia-Romagna coastal plain are characterised by the cyclical organisation of marine and continental deposits in succession of various hierarchical order, for a thickness of several hundred metres. In the study area, two main depositional cycles are identified, defined as Qm and Qc, whose discontinuity surface is at the boundary between the Supersynthem of the Marine Quaternary, corresponding to the Qm cycle, and the overlying Emiliano - Romagnolo Supersynthem, equivalent to the Qc cycle (Ricci Lucchi *et al.*, 1982; Di Dio, 1998; Preti, 2002). The Emiliano - Romagnolo Supersynthem is divided into the Lower Emiliano - Romagnolo Synthem - AEI and the Upper Emiliano - Romagnolo Synthem - AES, both ca. 300 m thick. Studies based on the interpretation of seismic profiles integrated by well data provided a general stratigraphic framework of the Quaternary deposits in the Ravenna area, showing that the Emiliano - Romagnolo Supersynthem has in this sector of the plain a total thickness of about 600-700 m (Di Dio, 1998; Preti, 2002).

According to Carminati *et al.* (2003a), a significant amount of the natural subsidence in the study area is related to the flexure of the Adriatic plate due to its subduction. Sediment load/compaction and deglaciation-related ice melting also contribute to natural subsidence (Carminati *et al.*, 2003a). The onshore (along coast) total natural subsidence rates in the study area were estimated to be around 3 mm/yr (Carminati *et al.*, 2003b). The difference between present-day subsidence rates from geodetic data and this subsidence rate from geological data can be used to evaluate the effects of anthropic activities (Severi *et al.*, 2021).

### 3. Materials, methods and preliminary results

In this paragraph, the data and the methods exploited to investigate subsidence affecting the area of study are presented. In particular, in section 3.1 the *in situ* data provided by the Emilia-Romagna Region and Regional Agency for the Environmental Protection and Energy (ARPAE Emilia-Romagna), such as geological and structural maps, piezometric measurements, underground water withdrawal volumes, etc., are listed and detailed. In the subsequent section 3.2, the numerical simulations carried out by a 3D fluid-dynamic and geomechanical modelling based on these data are presented. Finally, in section 3.3 the description of the used satellite data, the processing technique, the performed DInSAR analysis, and the achieved results, is reported.

#### 3.1. Description of *in situ* data

The Emilia-Romagna Region and ARPAE Emilia-Romagna have provided the following data set for the study area (blue polygon in Fig. 1):

- cartographic basemaps: topographic map, geologic and structural maps, the latter specifically processed for the case study;
- 14 deep geological and hydrogeological cross-sections (7 from ISPRA, 1988);
- 612 geologic surveys from geognostic database of the Emilia-Romagna Region that provided different information (e.g. location, depth, lithological pattern). This database includes several static penetrometric tests [Cone Penetration Test (CPT)], for which the raw parameters and some elaborations as Robertson's parameters are provided (Robertson, 2009; Robertson and Cabal, 2014);
- 106 surveyed groundwater withdrawal wells classified for function and use (civil, industrial, irrigation, livestock) with the corresponding volumes of water ( $\text{Mm}^3/\text{yr}$ ) annually produced by the wells. These data are available for the following years: 1975, 1990, 2000, 2010, and 2017 (Figs. 2 and 3);
- 12 piezometers, belonging to the Regional Groundwater Monitoring Network with the relative piezometric measurements carried out over time. The frequency of piezometric measures changes from well to well, so it is not uniform and can be annual or monthly (note that experimental piezometric data are not available between 1998 and 2002 as reported in Fig. 4).

#### 3.2. Numerical simulations: fluid-dynamic and geomechanical modelling

The data described in the previous section (like stratigraphy, well data, etc.) were imported in Petrel™ software (Schlumberger Ltd, 2016) and were processed and used for the 3D modelling. The elaboration of the 3D geological model was used to perform fluid-dynamic simulations aimed to define the effects induced on the surface by the groundwater withdrawal. The code used for the fluid-dynamic modelling was Tough2 (Pruess, 1990) integrated in GeoSIAM - Integrated System of Analysis for geomodelling developed by RSE (Agate and Guandalini, 2018); the geomechanical modelling was performed with PyLith code (Aagaard, *et al.*, 2013, 2017). In detail, to define the interface surfaces of geologic units in Petrel, well data were analysed together with the available geological and hydrogeological cross-sections to define petrophysical parameters.

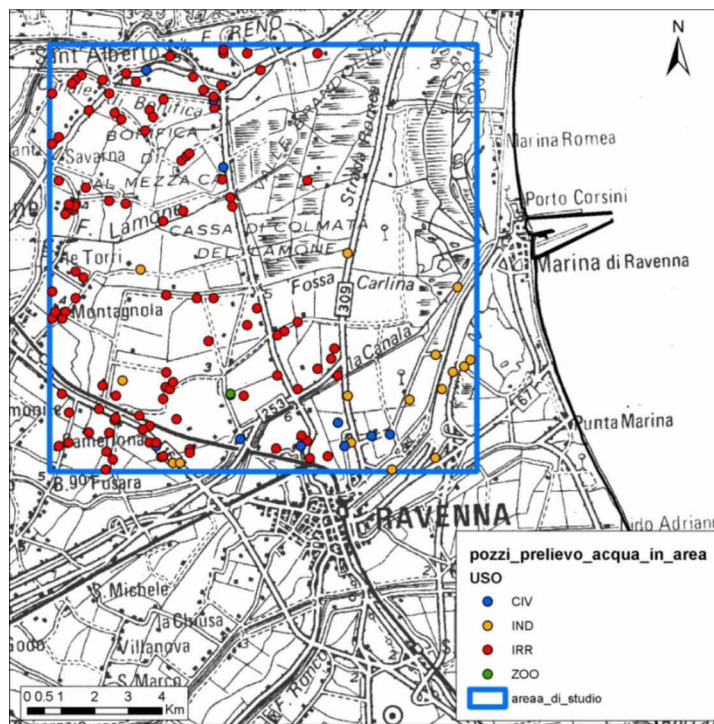


Fig. 2 - Location of groundwater withdrawal wells in the study area (blue polygon) classified for use and function (yellow for industrial, red for irrigation, blue for civil, green for livestock) (data from Regional Agency for the Environmental Protection and Energy - ARPAE Emilia-Romagna).

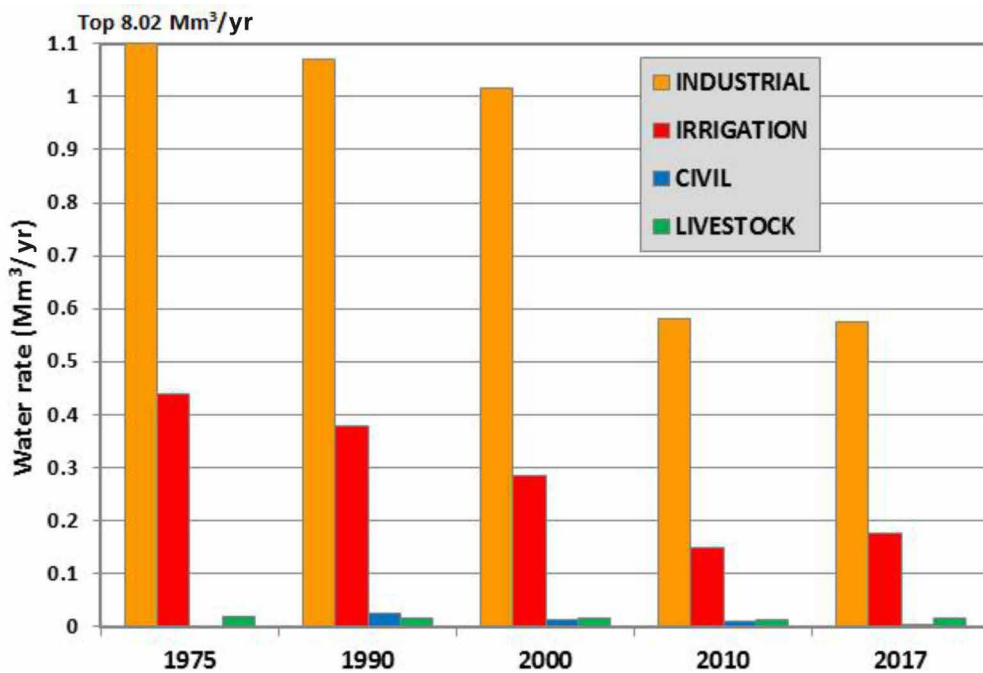


Fig. 3 - Volumes (Mm³/yr) of groundwater withdrawal in the study area classified for use and function (yellow for industrial, red for irrigation, blue for civil, green for livestock) (data from Regional Agency for the Environmental Protection and Energy - ARPAE Emilia-Romagna).

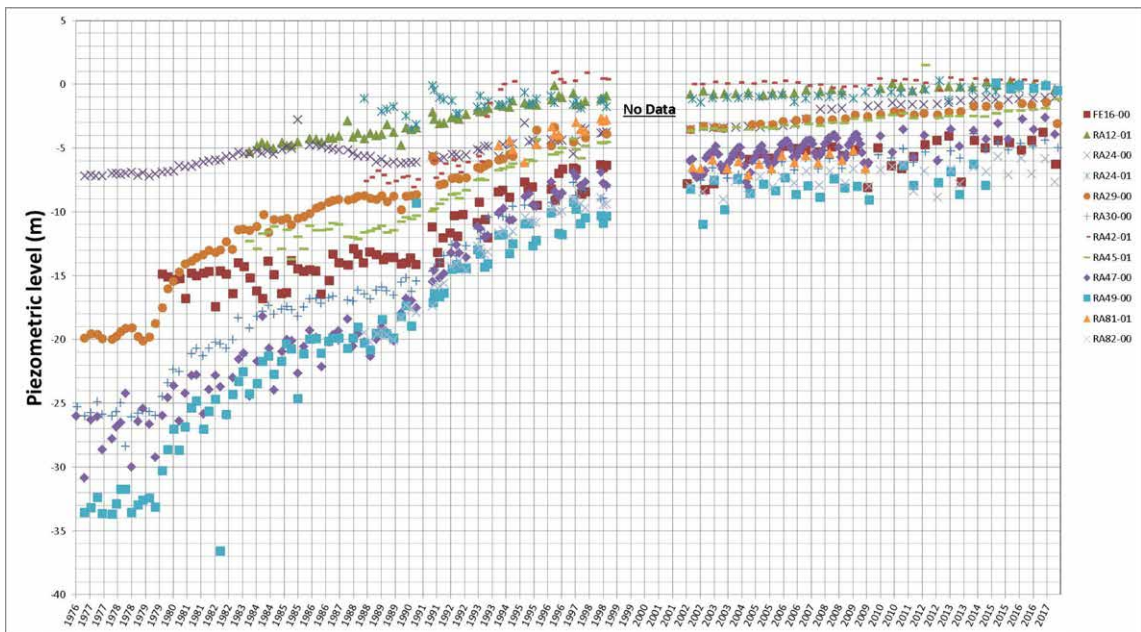


Fig. 4 - Piezometric trend recorded during the 1976-2017 period from wells located in the study area. This chart highlights the build-up of piezometric level during time when the water volumes withdrawal decremented. Data are not available for the 1998-2002 period (data from ARPAE Emilia-Romagna).

A 3D dynamic grid was created with dimensions of approximately  $12.5 \times 12.5$  km<sup>2</sup> in the  $x$  and  $y$  directions and -400 m of depth in  $z$  direction. This 3D dynamic grid was carried out by following the Voronoi tessellation method (Voronoi, 1909; Okabe *et al.*, 2010; Mei, 2014) implemented in GeoSIAM software with each element of the grid consisting of a 3D polygonal element with a maximum of 20 sides. This type of computational grid has the advantage of having the connection sides orthogonal to the mass centre connectors as required by the method of discretisation to integral finite differences used by the Tough2 simulator (Pruess, 1990). The geometry of the 106 examined wells for water production was integrated into the dynamic grid and a grid refining was carried out near the wells creating 3D concentric rings of 8 elements each around the wells. The geological and structural characteristics of this investigated area were subdivided into 98 vertical layers whose thickness ranges between 3 and 10 m; therefore, the final 3D dynamic grid consists of 463,050 elements, 745,173 nodes and 1,652,651 connections. During the grid generation phase, the pertinent petrophysical properties derived from the geological and lithological characteristics of the area were attributed to each cell and are summarised in Tables 1 and 2.

Before performing groundwater withdrawal simulations, an initialisation phase is required during which the wells are not active and thus reproduction of the correct initial pressure and temperature distribution is allowed within the calculation domain. Then, using the geological model and computational grid described above, groundwater drainage simulations were performed for the 5 years with full availability of experimental data (1975, 1990, 2000, 2010, and 2017) and the annual pressure difference between initial and final state of groundwater withdrawal was estimated. This pressure difference represents the input force for the geomechanical simulation and the vertical subsidence estimation related to the groundwater withdrawal from superficial aquifers.

The geomechanical numerical simulation was carried out using the PyLith software and the 3D dynamic grid was transformed into a hexahedral 3D grid necessary to operate with a finite element software. For finite element grid generation, a subdivision of elements with the same geomechanical properties was carried out and the final 3D grid consists of 33 vertical layers, 180,048 cells, and 186,898 nodes.

To better understand the magnitude of subsidence process, further simulations were performed using 3 different rock compressibility values to cover the variability range for the available experimental values and the results of the numerical simulations are reported in Table 3. Maps of vertical displacement ( $z$  axis) obtained considering the average compressibility values for the study area in 2000, 2010, and 2017 are shown in Fig. 5. The uncertainties associated with the deformation results retrieved via the numerical simulations depends on numerous factors that requires an in depth analysis. However, preliminary results using as example a different discretisation of the mesh produced no appreciable differences on the simulations.

Table 1 - Geomechanical parameters used for the study.

Parameter [unit]	Symbol	Sand	Clay
Poisson's coefficient [-]	$\nu$	0.3	0.3
Young's modulus [Pa]	$E$	2.00 E+09	2.18E+07
Porosity [-]	$\varepsilon_f$	0.35	0.07
Permeability [m <sup>2</sup> ]	$k$	9.09E-13	1.00E-14
Density [kg/m <sup>3</sup> ]	$\rho$	1.90E+03	1.90E+03
Biot coefficient ( $\alpha = \varepsilon_p$ ) [-]	$a$	0.35	0.07
Vertical compressibility [Pa <sup>-1</sup> ]	$m_v$	6.00E-10	5.50E-08
Pores compressibility [Pa <sup>-1</sup> ]	$\beta_p = mv/ef$	1.71E-09	7.86E-07
Bulk modulus [Pa]	$K$	1.67E+09	1.82E+07
Confined modulus [Pa]	$M$	2.69E+09	2.94E+07
Tangential modulus [Pa]	$G = \mu$	7.69E+08	8.39E+06

Table 2 - Different compressibility values ( $z$  axis oriented upwards): lower, average and upper values for sand and clay.

Parameters [unit]	Sand			Clay		
	Average value	Lower value	Upper value	Average value	Lower value	Upper value
Vertical compressibility [Pa <sup>-1</sup> ]	6.00E-10	3.00E-10	9.00E-10	5.50E-08	1.00E-08	1.00E-07



Table 3 - Simulated maximum vertical displacement in mm recorded at surface in different years (1975, 1990, 2000, 2010, and 2017) for different compressibility values in Table 2 ( $z$  axis oriented upwards).

	Maximum vertical displacement values retrieved via numerical simulations [mm]				
	1975	1990	2000	2010	2017
Average compressibility value (see Table 2)	- 2.87	- 1.65	- 1.62	- 0.92	- 0.98
Lower compressibility value (see Table 2)	- 2.55	- 1.56	-1.49	- 0.93	- 0.93
Upper compressibility value (see Table 2)	- 4.16	- 2.44	- 2.30	- 1.34	- 1.33

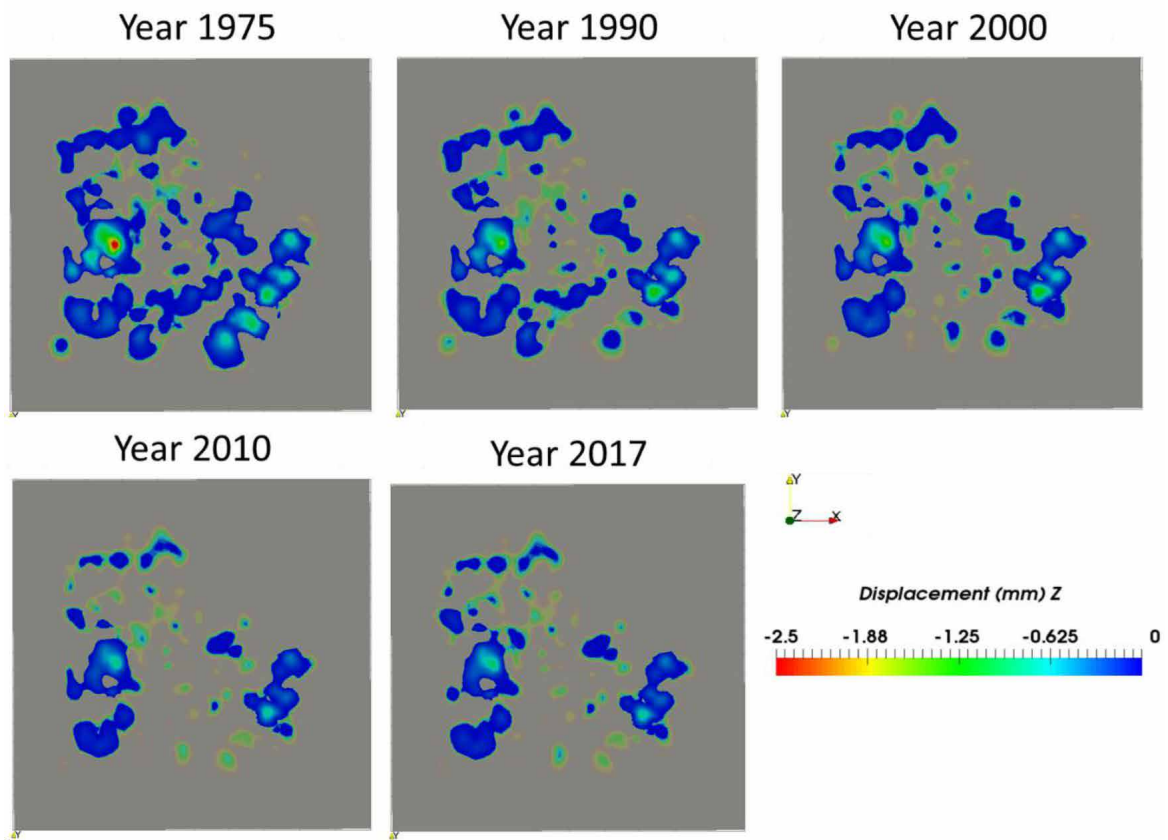


Fig. 5 - Maps of the simulated vertical displacement (in mm) relevant to the average compressibility values of Table 2 for years 1975, 1990, 2000, 2010, and 2017.

### 3.3. DInSAR analysis

The ground deformation affecting the investigated area has been deeply analysed by using the satellite remote sensing technique referred to as DInSAR technique (Gabriel *et al.*, 1989; Massonet *et al.*, 1993) that allows the generation of spatially dense ground deformation

maps with centimetre to millimetre accuracy. This is done by analysing the phase difference (interferogram) of two temporally separated SAR images, with the measured displacements representing the projection of the surface deformation on the radar Line Of Sight (LOS). The results presented in this study are retrieved by applying the advanced DInSAR algorithm referred to as Small BAseline Subset (SBAS) approach (Berardino *et al.*, 2002), that allows following the temporal evolution of the detected deformation phenomena via the generation of displacement velocity maps and corresponding time series relevant to the whole period of observation. In particular, the SBAS approach implements an easy combination of the differential SAR interferograms generated from an appropriate selection of SAR data pairs characterised by a small spatial and temporal separation (baseline) between the acquisition orbits in order to mitigate the noise effects (Zebker and Villasenor, 1992) and on the application of the Singular Value Decomposition (SVD) method. The latter is applied to the set of multilooked (Rosen *et al.*, 2000) and unwrapped (Pepe *et al.*, 2015) interferograms and allows linking independent SAR acquisition data sets separated by large spatial baselines, thus increasing the number of data used for the analysis. Moreover, this technique includes a step for the detection and removal of orbital fringes, topography-related contributions and atmospheric phase components (Berardino *et al.*, 2002).

In this study, the following four sets of C-band SAR data, acquired from ERS/ENVISAT, and Sentinel-1 sensors were considered:

1. 70 ERS-1/2 and ENVISAT SAR data acquired from ascending orbits (track 172) in the June 1995 - July 2010 time interval;
2. 138 ERS-1/2 and ENVISAT SAR data acquired from descending orbits (track 122) in the May 1995 - July 2010 time interval;
3. 166 Sentinel-1 SAR data acquired from ascending orbits (track 117) in the March 2015 - December 2018 time interval;
4. 171 Sentinel-1 SAR data acquired from descending orbits (track 95) in the March 2015 - December 2018 time interval.

The related differential interferograms were computed for each data set by exploiting the 1-arcsec STRM (Shuttle Radar Topography Mission) DEM (Digital Elevation Model) of the study area; in addition, a complex multilook operation, resulting in a pixel size of approximately 80×80 m<sup>2</sup>, was performed. Moreover, to each SAR data set the SBAS technique was applied (Berardino *et al.*, 2002; Pepe *et al.*, 2005; Casu *et al.*, 2014; Manunta *et al.*, 2019) and the LOS mean deformation velocity maps and the corresponding time series for each coherent pixel (i.e. the pixels where the noise effects can be assumed negligible) identified in the imaged scene were generated. In addition, the obtained results were referred to a (reference) pixel in the centre of the city of Ravenna, close to the Giardini Pubblici.

By benefitting from the availability of DInSAR measurements from both ascending and descending radar LOS, the vertical and E-W mean velocity components (Manzo *et al.*, 2006) for the pixels common to both radar geometries were estimated. Accordingly, the mean vertical deformation velocity maps for the ERS/ENVISAT (1995-2010) and Sentinel-1 (2015-2018) SAR data were generated and reported in Figs. 6a and 6b, respectively. Fig. 6 shows these maps (colour scale) superimposed on the DEM (grey scale) of the area, wherein low coherence zones are masked out. This kind of representation is particularly effective because it provides direct information on the estimated mean deformation rate. Both maps reveal that the whole city of Ravenna is quite stable without showing significant velocity rates; only the agricultural zone SE of the study area

shows a subsidence pattern with values up to  $-6/-7$  mm/yr (see Fig. 6b). The surrounding zone, NW of study area, exhibits a poor coherent pixel density (and this is more evident for the ERS/ENVISAT results with respect to the Sentinel-1 ones, see Fig. 6); this occurs essentially due to the characteristics of the exploited C-band SAR systems that do not preserve coherence over time in vegetated/agricultural areas. Moreover, both maps show subsidence patterns involving the coastal areas, particularly those south of Marina di Ravenna with values up to  $-13$  mm/yr for the ERS/ENVISAT data and up to  $-15$  mm/yr for the Sentinel-1 ones. In addition, also the industrial area (between Ravenna and Marina di Ravenna) and the harbour of Ravenna city are affected by subsidence with velocity rates also exceeding  $-20$  mm/yr (see Fig. 6b). It is worth noting that the Sentinel-1 vertical velocity map presents a coherent pixel density significantly improved with respect to that of the ERS/ENVISAT one. This is mostly related to both the revisit-time reduction and the orbital tube narrowness of the Sentinel-1 sensors with respect to those of the ERS/ENVISAT sensors [6 days vs. 35/70 days and 200 m vs. 2000 m, respectively, Manunta *et al.* (2019)]. Furthermore, it is important to underline that the Sentinel-1 results are relevant to the ground displacements where the low spatial frequency component, essentially induced by regional tectonic, was removed; accordingly, they provide information on the high spatial frequency component related to deformation phenomena. This operation was carried out by following the lines discussed in Lanari *et al.* (2020) and by using the continuous GPS position time series provided by the Nevada Geodetic Laboratory at the University of Nevada, Reno, USA (UNR-NGL) (Blewitt *et al.*, 2018) in the framework of the “Plug and Play GPS” project. Such a project takes the raw GPS data from more than 17,000 stations all around the world and makes publicly available via a web-site (<http://geodesy.unr.edu>) the related data products for all the geodetic quality GPS stations. For what concerns the investigated area, we remark that it represents a very small portion of the entire processed Sentinel-1 frame (that covers an area of about  $300 \text{ km} \times 250 \text{ km}$ ). Overall, we used the position time series relevant to 52 GPS stations; they are those returned by a proper selection and screening operation carried out on the 83 stations deployed within the entire frame (Lanari *et al.*, 2020). These GPS measurements were considered to compute the GPS-derived regional deformation pattern used within the velocity calibration procedure that finally provides high spatial frequency deformation components (Lanari *et al.*, 2020).

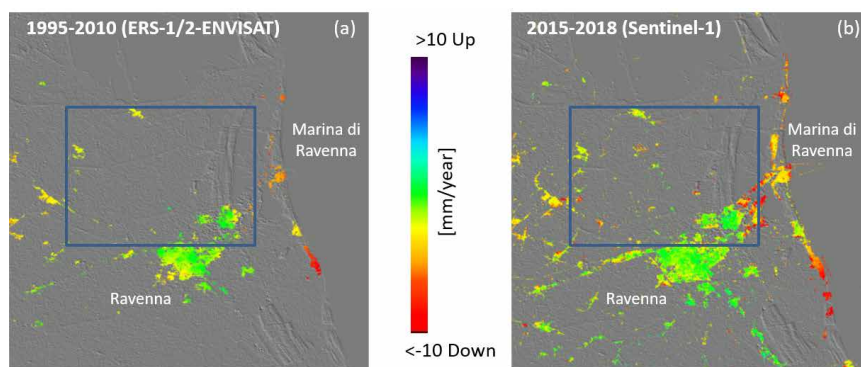


Fig. 6 - DInSAR analysis results. Mean deformation vertical velocity maps (mm/yr) computed in coherent areas and superimposed on the DEM of the investigated zone: a) results relevant to the ERS/ENVISAT SAR data for the 1995-2010 time interval; b) results relevant to the Sentinel-1 SAR data for the 2015-2018 time interval. The blue polygon identifies the study area in the Ravenna onshore.

Availability of vertical deformation temporal time series (Casu and Manconi, 2016) allowed, besides, the computation of the vertical cumulative displacements for three selected periods and for the area of study (previously identified via the blue rectangles in Fig. 6). Figs. 7a, 7b, and 7c show the vertical displacement cumulative maps (colour scale) for the investigated area, superimposed on the DEM (grey scale) of the zone, for the 2000, 2010, and 2017 periods, respectively. Note that the 2000 and 2010 maps were obtained from the ERS/ENVISAT SAR data, while the 2017 one from the Sentinel-1 measurements. Note, also, that these three periods were selected, among those investigated through the groundwater withdrawal fluid-dynamic modelling (Fig. 5), since they are the ones for which SAR data were available (i.e. no SAR data was acquired before 1990). These maps were computed by considering for each coherent pixel the linear regression that best fits the related time series within the selected periods. Accordingly, the corresponding mean vertical deformation velocities were obtained and used to retrieve the vertical deformation for the year of interest.

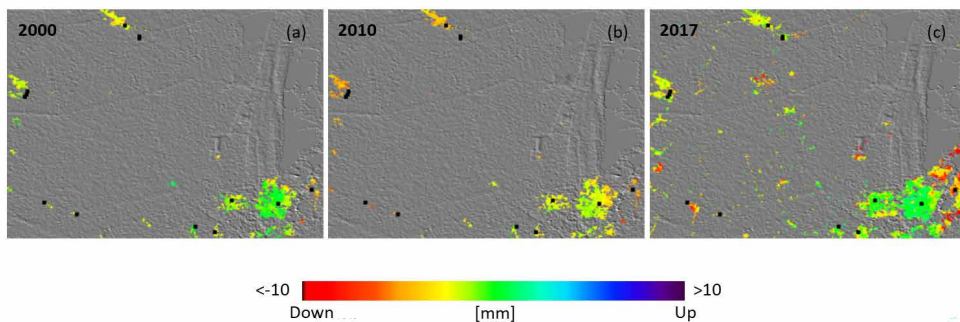


Fig. 7 - DInSAR analysis results for the area of study (see blue polygon in Fig. 6). Vertical cumulative displacement maps (mm) for three time intervals, computed in coherent areas and superimposed on the DEM of the investigated zone: a) year 2000 from ERS/ENVISAT SAR data; b) year 2010 from ERS/ENVISAT SAR data; c) year 2017 from Sentinel-1 SAR data. The black squares identify the 13 wells used for the DInSAR analysis/numerical simulations comparison.

Starting from these maps, the DInSAR vertical deformation at wells were computed. In particular, 13 of the 106 original wells used in the fluid-dynamic and geomechanical modelling were considered for both the ERS/ENVISAT and Sentinel-1 DInSAR results. These wells are located in zones that are coherent in both the ERS/ENVISAT and Sentinel-1 DInSAR displacement maps; moreover, they are those that present significant displacements as revealed by the fluid-dynamic simulations. For each year, the DInSAR vertical deformation in correspondence to the coherent pixels located inside a well-centred box, extending approximately  $500 \times 500 \text{ m}^2$ , was considered. Subsequently, for each box the vertical deformation of the corresponding coherent pixels was averaged, thus obtaining a mean deformation value for each considered well. Finally, for each year an overall mean deformation vertical value was evaluated, by averaging the so-computed vertical displacement values at the 13 selected wells. The results of this analysis are reported in Table 4. Moreover, in order to provide an estimate of the mean vertical deformation relevant to the whole area of study (and not limited to the 13 well sites), the mean vertical displacement values for all the ERS/ENVISAT and Sentinel-1 coherent pixels located within this area were computed (thus, significantly increasing the number of pixels used for this analysis, now considering some/tens of thousands of pixels). Also, these values are reported in Table 4. The results (Fig. 7 and Table 4) are discussed in the following paragraph, also by comparing them to those retrieved through the numerical simulations (section 3.2).

Table 4 - Averaged vertical displacement values (in mm) measured for the 2000, 2010, and 2017 years retrieved via DInSAR analysis.

	Averaged vertical displacement values retrieved via DInSAR analysis [mm]		
	2000	2010	2017
13 wells	- 2.1	- 4.4	- 2.6
ERS/ENVISAT coherent pixels	- 1.3	- 3.2	
Sentinel-1 coherent pixels			- 2.3

#### 4. Discussion

On the basis of the results presented in the previous sections, the discussion will be organised in three main topics:

- vertical displacement around water withdrawal wells retrieved via the SBAS-DInSAR technique for years 2000, 2010, and 2017;
- comparison and discussion of the results from the two techniques used in this work;
- total subsidence in the study area considering the SAR data processed via the SBAS-DInSAR technique (1995-2018).

Concerning the first topic, a general total subsidence rate in the study area of up to -13 mm/yr for the ERS/ENVISAT data (1995-2010) and up to -15 mm/yr for the Sentinel-1 (2015-2018) is estimated. These values include both natural and anthropogenic causes where the total natural subsidence rates in the study area is estimated to be around 3 mm/yr by Carminati *et al.* (2003b).

Furthermore, the DInSAR analysis presented in section 3.3 provided the total subsidence for the years 2000, 2010, and 2017 and, in particular, around the 13 wells located in the study area and selected considering those with significant vertical displacement, as suggested by the numerical simulations. The results of this analysis, reported in Fig. 7 and Table 4, reveal an increase of the subsidence (in absolute value) from year 2000 to 2010 and a decrease from year 2010 to 2017. This is evident by analysing the vertical displacement maps of Fig. 7. Moreover, this subsidence pattern is also evident by computing the averaged vertical deformation values for the three years, by performing both the analysis based on the DInSAR coherent pixels located at the 13 wells and the one based on all the coherent DInSAR pixels included in the area of study. Indeed, both analyses show similar findings, i.e. mean vertical deformation values increase (in absolute value) passing from 2000 to 2010, and then decrease passing from 2010 to 2017.

Regarding the second topic, by jointly analysing the results derived from the two methods, at local scale, considering 13 wells of those present in the study area, it is possible to estimate the contribution of ground water extraction over the total subsidence by comparing Tables 3 and 4. Considering the values in the two tables, and in particular the results in Table 3 corresponding to average compressibility value (similar considerations, although characterised with different values), can be obtained by considering the upper and lower compressibility values), it is visible that the contribution of ground water extraction in the three years 2000, 2010, and 2017 changes from 79% in 2000 to 21% in 2010 and to 38% in 2017. This is in line with the information derived by data of groundwater volume extraction that show a big reduction from  $8.48 \cdot 10^6$  m<sup>3</sup>/yr in 1975 to  $0.77 \cdot 10^6$  m<sup>3</sup>/yr in 2017. However, while is mostly true for period 1975 to 2000, it seems to partially differ for the period from 2010 to 2017 when the performed joint analysis suggests a decrease of subsidence resulting in a major contribution of groundwater withdrawal, not confirmed by the volume extracted.

Furthermore, in the period 2000–2010, in the study area the presented analysis shows an increase of subsidence due to water withdrawal and other components. Such a difference could be explained considering other causes of compaction, such as major loading of buildings/infrastructure especially in the Ravenna canal/harbour zone as observed through local investigation by Emilia Romagna Region. The retrieved values of the groundwater withdrawal to the total subsidence highlight that in the study area the contribution of groundwater withdrawal is larger than the one estimated by Regione Emilia-Romagna and ARPAE (2010) report that varies from 10 to 30%.

Therefore, it is possible that in the 2000–2010 period there was a delay effect due to decrease in the extracted groundwater volume, as Teatini *et al.* (2006) report: “Land subsidence near the coast during 1977–2001, a period when aquifer pore pressure was increasing, results from delayed consolidation of the aquitards. Moreover, the virgin aquifer compaction ended in 1977 and the subsequent elastic reaction in unloading conditions accounts for an only partial recovery of the original deformation”.

For the 2010–2017 period, the performed analysis seems to indicate a partial recovery of the total subsidence with decreasing vertical displacements and a larger contribution of groundwater withdrawal to the total subsidence, moving from 21% to 38%, despite a stabilisation of the extracted water volumes, also thanks to good management policies adopted from 2000 onwards.

Finally, concerning the third topic, we remark that the DInSAR analysis has been carried out by considering two separate time intervals, i.e. 1995–2010 and 2015–2018. For both periods we find that the whole city of Ravenna is quite stable without showing significant velocity rates and that the agricultural zone SE of the study area shows a subsidence pattern with values up to  $-6$  to  $-7$  mm/yr. Moreover, the industrial area (between Ravenna and Marina di Ravenna) and the harbour of Ravenna city result to be affected by subsidence with velocity rates also exceeding  $-20$  mm/yr within the two time intervals. In addition, the coastal areas, particularly those south of Marina di Ravenna, are interested by subsidence with values up to  $-13$  mm/yr for the 1995–2010 period and up to  $-15$  mm/yr for the 2015–2018 one. This slight difference can be due to several aspects related both to the different characteristics of the employed SAR data (i.e. for the 2015–2018 the SAR systems allow better monitoring with respect to the 1995–2010 one the agricultural/coastal areas; accordingly, an increased number of pixels can be observed) and to natural phenomena and/or man-made activities that may be changed over time (compaction processes, soil exploitation, etc.). Finally, we outline that the DInSAR results presented in this work, relevant to the mean vertical deformation velocities in the Ravenna onshore study area, were computed with different methodologies with respect to other studies from the literature (Regione Emilia-Romagna and ARPAE, 2007, 2018). The different interferometric analyses are not easily comparable for several factors. The used SAR data set are referred to different periods (Regione Emilia-Romagna and ARPAE reports: 1992–2000, 2002–2006, 2011–2016, this study: 1995–2010, 2015–2018) and influence the estimate of the mean deformation velocity, above all if the ground displacements are not linear in the whole period of observation. DInSAR data were processed with two different techniques (PS and SqueeSAR in the Regione Emilia-Romagna and ARPAE reports, SBAS in this study). In the cited reports, SAR data collected from one single acquisition geometry (ascending or descending) were used, except for the 2002–2006, when both acquisition geometries were considered. Instead, this study is totally based on the double geometry. The interferometric analysis for the 2011–2016 (Regione Emilia-Romagna and ARPAE, 2018) and the 2015–2018 (this study) time intervals have benefitted from a different use of GPS measurements to calibrate the retrieved DInSAR results in order to detect the regional signal-related component. The 2011–2016 DInSAR results (Regione Emilia-Romagna and ARPAE, 2018) provide an image of the general deformation phenomena affecting the whole region, while the 2015–2018 DInSAR presented in this study provide information on local deformation phenomena affecting a small portion of the region, obtained by removing the regional signal-related from DInSAR results. Furthermore, the number and position of GPS measurements exploited by both interferometric analyses is significantly different. In particular, 16 GPS stations deployed in the whole

Emilia-Romagna region for the 2011-2016 report (Regione Emilia-Romagna and ARPAE, 2018) were used, while for the 2015-2018 study we exploited 52 stations located in an area that only partially overlaps with that of the 2011-2016 report [for more details see Lanari *et al.* (2020)]. Finally, the spatial extension of the investigated area and the SAR reference, just to mention some of the several aspects involved in the interferometric analysis, can also contribute to the retrieved differences.

## 5. Conclusions

Subsidence represents the final effect of a regional geodynamic and tectonic and local compaction processes. Compaction processes can have natural or anthropogenic causes as, for example, the filling of a sedimentary basin, the withdrawal of groundwater or the oil and gas production. The CLYPEA programme, within the project “Ground deformation” (Antoncecchi *et al.*, 2018), proposed the integration of different approaches for the investigation of subsidence in the Emilia-Romagna Region area located between Comacchio, to the north, and Ravenna, to the south. In this work, the fluid-dynamic and geomechanical 3D modelling simulated the contribution of the groundwater production to the total detected deformation due to groundwater withdrawal [within 400 m below the surface by using data of compressibility available from literature, see Regione Emilia-Romagna and ARPAE (2010) report] for 5 years - 1975, 1990, 2000, 2010, and 2017, when data of the extracted groundwater volumes were statistically significant. Moreover, SAR data from ERS/ENVISAT and Sentinel-1 sensors were processed through the SBAS technique and provided information on the total subsidence affecting the area of study for the 1995-2018 period.

The study highlights the advantages of a multi-disciplinary approach to deeply investigate the subsidence process occurring in the area of study, and that typically affects the Emilia-Romagna region. The contribution of groundwater withdrawal in the three considered years 2000, 2010, and 2017 changes from 79% in 2000, to 21% in 2010, and 38% in 2017. This is generally in line with groundwater withdrawal data that show a reduction of the extracted water volumes during the considered temporal interval. Accordingly, this contribution to the total subsidence results to be larger with respect to the estimates of Regione Emilia-Romagna and ARPAE (2010) that span from 10% to 30%. Moreover, the joint analysis shows that a delay effect in the subsidence process, as response to a decrease in the extracted groundwater volumes is detected for the 2000-2010 period; a partial recovery of this process seems to occur during the 2010-2017 interval when a stabilisation of the extracted groundwater volumes was imposed.

The presented results bring new evidence about the contribution of groundwater withdrawal to the total subsidence in the study area. These results need further investigations through future researches that must benefit of integrated approaches exploiting proper continuous spatial and temporal data set for satellite, geological, and production data (e.g. water withdrawal volumes).

**Acknowledgments.** This study is performed under the umbrella of “CLYPEA - Innovation Network for Future Energy” promoted and financed by the Italian Ministry of Economic Development - DG ISSEG, in the framework of the project “Subsoil deformations” made in collaboration with Research on Energy System - RSE, National Institute of Geophysics and Volcanology - INGV, University of Bologna, Polytechnic of Turin, Sapienza University, National Research Council - IGAG and National Research Council - IREA, and Emilia-Romagna Region. DInSAR data processing is also partially sponsored by the I-AMICA project (PONa3 00363). We thank the Emilia-Romagna Region for sharing historical data and knowledge about the study area. Thanks also to the European Space Agency for providing the ERS/ENVISAT ASAR data, and to the NASA SRTM mission for the DEM of the analysed area. Sentinel-1 data were provided through the Copernicus Program of the European Union.

## REFERENCES

- Aagaard B.T., Knepley M.G. and Williams C.A.; 2013: *A domain decomposition approach to implementing fault slip in finite element models of quasi statics and dynamic crustal deformation*. J. Geophys. Res.: Solid Earth, 118, 3059-3079, doi: 10.1002/jgrb.50217.
- Aagaard B.T., Knepley M.G. and Williams C.A.; 2017: *Geodynamics/pylith: PyLith v2.2.1, (Version v2.2.1)*. Zenodo, doi: 10.5281/zenodo.886600.
- Agate G. and Guandalini R.; 2018: *Manuale d'uso del software GeoSIAM versione 2.0*. RSE 18002366, RSE S.p.A., Milano, Italy.
- Amadori C., Garcia-Castellanos D., Toscani G., Sternai P., Fantoni R., Ghielmi M. and Di Giulio A.; 2018: *Restored topography of the Po Plain - Northern Adriatic region during the Messinian base-level drop - Implications for the physiography and compartmentalization of the palaeo-Mediterranean basin*. Basin Res., 30, 1247-1263, doi: 10.1111/bre.12302.
- Amorosi A., Colalongo M.L., Pasini G. and Preti D.; 1999: *Sedimentary response to Late Quaternary sea level changes in the Romagna coastal plain (northern Italy)*. Sedimentology, 46, 99-121.
- Antoncecchi I., Rossi G., Ciccone F., Carminati E., Morelli A., Pezzo G., Macini P., Gandolfi S., Lanari R., Manzo M., Moia F., Verga F., Perini L., Severi P., Petracchini L., Billi A. and Terlizze F.; 2018: *Studio multidisciplinare per la valutazione delle deformazioni del suolo connesse alle attività di produzione di idrocarburi in aree dell'offshore emiliano romagnolo finalizzato allo sviluppo di un modello per il monitoraggio finalizzato*. In: Gruppo Nazionale di Geofisica della Terra Solida, 37° Convegno Nazionale, Riassunti estesi delle comunicazioni, Centro Stampa della Regione Emilia Romagna, pp. 501-504.
- Benetatos C., Codegone G., Deangeli C., Giani G., Gotta A., Marzano F., Rocca V. and Verga F.; 2017: *Guidelines for the study of subsidence triggered by hydrocarbon production*. GEAM - Geoingegneria Ambientale e Mineraria, 152, 85-96.
- Benetatos C., Codegone G., Ferraro C., Mantegazzi A., Rocca V., Tango G. and Trillo F.; 2020: *Multidisciplinary analysis of ground movements: an underground gas storage case study*. Remote Sens., 12, 3487, doi: 10.3390/rs12213487.
- Berardino P., Fornaro F., Lanari R. and Sansosti E.; 2002: *A new algorithm for surface deformation monitoring based on small baseline differential SAR interferograms*. IEEE Trans. Geosci. Remote Sens., 40, 2375-2383.
- Bertoni W., Brighetti G., Gambolati G., Ricceri G. and Vuillemin F.; 1995: *Land subsidence due to gas production in the on- and off-shore natural gas fields of the Ravenna area, Italy*. IAHS Publ., 234, 13-20.
- Bissoli R., Bitelli G., Bonsignore F., Rapino A. and Vittuari L.; 2010: *Land subsidence in Emilia-Romagna Region, northern Italy: recent results*. IAHS Publ., 339, 307-311.
- Blewitt G., Hammond W.C. and Kreemer C.; 2018: *Harnessing the GPS data explosion for interdisciplinary science*. Eos, 99, doi: 10.1029/2018EO104623.
- Calabrese L., Luciani P. and Perini L.; 2021: *A review of impact of subsidence induced by gas exploitation on coastal erosion in Emilia-Romagna, Italy*. Boll. Geof. Teor. Appl., 62, 279-300, doi: 10.4430/bgta0356.
- Carminati E. and Martinelli G.; 2002: *Subsidence rates in the Po Plain (northern Italy): the relative impact of natural and anthropic causation*. Eng. Geol., 66, 241-255.
- Carminati E., Wortel M.J.R., Spakman W. and Sabadini E.R.; 1998: *A new model for the opening of the western central Mediterranean basins: geological and geophysical constraints for a major role of slab detachment*. Earth Planet. Sci. Lett., 160, 651-665.
- Carminati E., Doglioni C. and Scrocca D.; 2003a: *Apennines subduction related subsidence of Venice (Italy)*. Geophys. Res. Lett., 30, 1717, doi: 10.1029/2003GL017001.
- Carminati E., Martinelli G. and Severi P.; 2003b: *Influence of glacial cycles and tectonics on natural subsidence in the Po Plain (northern Italy): insights from 14C ages*. Geochem. Geophys. Geosyst., 4, 1082-1096.
- Carminati E., Doglioni C. and Scrocca D.; 2005: *Magnitude and causes of long-term subsidence of the Po Plain and Venetian region*. In: Fletcher C.A. and Spencer T. (eds), *Flooding and environmental challenges for Venice and its lagoon: state of knowledge*, Cambridge University Press, New York, NY, USA, pp. 21-28.
- Casu F. and Manconi A.; 2016: *Four-dimensional surface evolution of active rifting from spaceborne SAR data*. Geosphere, 12, 697-705, doi: 10.1130/GES01225.1.
- Casu F., Elefante S., Imperatore P., Zinno I., Manunta M., De Luca C. and Lanari R.; 2014: *SBAS-DInSAR parallel processing for deformation time-series computation*. IEEE J. Sel. Top. Appl. Earth Obs. Remote Sens., 7, 3285-3296.
- Cenni N., Viti M., Baldi P., Mantovani E., Bacchetti M. and Vannucchi A.; 2013: *Present vertical movements in central and northern Italy from GPS data: possible role of natural and anthropogenic causes*. J. Geodyn., 71, 74-85.
- Coti C., Rocca V. and Sacchi Q.; 2018: *Pseudo-elastic response of gas bearing clastic formations: an Italian case study*. Energies, 11, 2488, doi: 10.3390/en11092488.



- Di Dio G. (a cura di); 1998: *Riserve idriche sotterranee della Regione Emilia - Romagna*. Regione Emilia-Romagna, Ambiente, Geologia, Sismica e Suoli and ENI S.p.A. - AGIP, Bologna, Italy, 120 pp.
- Doglioni C.; 1993: *Some remarks on the origin of foredeeps*. *Tectonophys.*, 228, 1-20.
- ENI and ARPAE; 2003: *Studio della subsidenza antropica generata dall'estrazione di acqua di falda lungo la costiera emiliano-romagnola*. ENI S.p.A. - AGIP and ARPAE Emilia-Romagna, Rapporto tecnico n. 4, 198 pp., <www.ARPae.it/cms3/documenti/subsidenza/Relfin\_Agip\_2003\_rid.pdf> (accessed on 13 June 2016).
- Ferretti A., Prati C. and Rocca F.; 2001: *Permanent scatterers in SAR interferometry*. *IEEE Trans. Geosci. Remote Sens.*, 39, 8-20.
- Fiaschi S., Tessitore S., Bonì R., Di Martire D., Achilli V., Borgstrom S., Ibrahim A., Floris M., Meisina C., Ramondini M. and Calcaterra D.; 2017: *From ERS-1/2 to Sentinel-1: two decades of subsidence monitored through A-DInSAR techniques in the Ravenna area (Italy)*. *GISci. and Remote Sens.*, 54, 305-328, doi: 10.1080/15481603.2016.1269404.
- Gabriel A.K., Goldstein R.M. and Zebker H.A.; 1989: *Mapping small elevation changes over large areas: differential interferometry*. *J. Geophys. Res.*, 94, 9183-9191.
- Gambolati G. (ed); 1998: *CENAS: coastal evolution of the upper Adriatic Sea due to sea level rise and natural and anthropogenic land subsidence*. Springer, Berlin, Germany, 359 pp.
- Gambolati G. and Teatini P.; 2015: *Geomechanics of subsurface water withdrawal and injection*. *Water Resour. Res.*, 51, 3922-3955, doi: 10.1002/2014WR016841.
- Gambolati G., Ricceri G., Bertoni W., Brighenti G. and Vuillermin E.; 1991: *Mathematical simulation of the subsidence of Ravenna*. *Water Resour. Res.*, 27, 2899-2918.
- Gambolati G., Teatini P., Tomasi L. and Gonella M.; 1999: *Coastline regression of the Romagna region, Italy, due to natural and anthropogenic land subsidence and sea level rise*. *Water Resour. Res.*, 35, 163-184.
- Ghielmi M., Minervini M., Nini C., Rogledi S., Rossi M. and Vignolo A.; 2010: *Sedimentary and tectonic evolution in the eastern Po-Plain and northern Adriatic Sea area from Messinian to Middle Pleistocene (Italy)*. *Rend. Lincei Sci. Fis. Nat.*, 21, 131-166.
- ISPRA; 1988: *CARG Project - Geologic and geothematic cartography*. <www.isprambiente.gov.it/en/projects/soil-and-territory/carg-project-geologic-and-geothematic-cartography>.
- Lanari R., Bonano M., Casu F., De Luca C.D., Manunta M., Manzo M., Onorato G. and Zinno I.; 2020: *Automatic generation of Sentinel-1 continental scale DInSAR deformation time series through an extended P-SBAS processing pipeline in a cloud computing environment*. *Remote Sens.*, 12, 2961, doi: 10.3390/rs12182961.
- Manunta M., De Luca C., Zinno I., Casu F., Manzo M., Bonano M., Fusco A., Pepe A., Onorato G., Berardino P., De Martino P. and Lanari R.; 2019: *The parallel SBAS approach for Sentinel-1 interferometric wide swath deformation time-series generation: algorithm description and products quality assessment*. *IEEE Trans. Geosci. Remote Sens.*, 57, 6259-6281, doi: 10.1109/TGRS.2019.2904912.
- Manzo M., Ricciardi G.P., Casu F., Ventura G., Zeni G., Borgstrom S., Berardino P., Del Gaudio C. and Lanari R.; 2006: *Surface deformation analysis in the Ischia island (Italy) based on spaceborne radar interferometry*. *J. Volcanol. Geotherm. Res.*, 151, 399-416, doi: 10.1016/j.jvolgeores.2005.09.010.
- Massonnet D., Rossi M., Carmona C., Ardagna F., Peltzer G., Feigl K. and Rabaute T.; 1993: *The displacement field of the landers earthquake mapped by radar interferometry*. *Nature*, 364, 138-142.
- Mei G.; 2014: *Summary on several Key techniques in 3D geological modelling*. *The Sci. World J.*, ID723832, 11 pp., doi: 10.1155/2014/723832.
- Okabe A., Boots B., Sugihara K. and Chiu S.N.; 2000: *Spatial tessellations: concepts and applications of Voronoi diagrams, 2nd ed.* John Wiley & Sons, Wiley Series in Probability and Statistics, Hoboken, NJ, USA, 696 pp.
- Pepe A., Sansosti E., Berardino P. and Lanari R.; 2005: *On the generation of ERS/ENVISAT DInSAR time-series via the SBAS technique*. *IEEE Geosci. Remote Sens. Lett.*, 2, 265-269.
- Pepe A., Yang Y., Manzo M. and Lanari R.; 2015: *Improved EMCF-SBAS processing chain based on advanced techniques for the noise-filtering and selection of small baseline multi-look DInSAR interferograms*. *IEEE Trans. Geosci. Remote Sens.*, 53, 4394-4417.
- Preti D. (a cura di); 2002: *Note illustrative della Carta Geologica d'Italia, foglio 223, Ravenna*. ISPRA, Servizio Geologico d'Italia - Regione Emilia Romagna, Roma, Italy, 141 pp.
- Pruess K.; 1990: *Tough2: a general purpose numerical simulator for multiphase fluid and heat flow*. Lawrence Berkeley Lab., CA, USA, Technical Report LBL-29400, 112 pp., doi: 10.2172/5212064.
- Regione Emilia-Romagna and ARPAE; 2007: *Rilievo della subsidenza nella pianura emiliano romagnola. Analisi interferometrica*. Regione Emilia-Romagna, Assessorato Ambiente e Sviluppo Sostenibile - Assessorato Sicurezza Territoriale, Difesa del Suolo e della Costa, Protezione Civile and ARPAE Emilia-Romagna, Agenzia Regionale Protezione Ambientale Energia, Bologna, Italy, 85 pp.

- Regione Emilia-Romagna and ARPAE; 2008: *Analisi preliminari degli effetti dei prelievi di acque sotterranee sull'evoluzione recente del fenomeno della subsidenza in Emilia-Romagna - Relazione Finale*. Regione Emilia-Romagna, Assessorato Ambiente e Sviluppo Sostenibile - Assessorato Sicurezza Territoriale, Difesa del Suolo e della Costa, Protezione Civile and ARPAE Emilia-Romagna, Agenzia Regionale Protezione Ambientale Energia, Bologna, Italy, 62 pp.
- Regione Emilia-Romagna and ARPAE; 2010: *Applicazione della modellistica matematica di simulazione. Fase II - Analisi della subsidenza nelle zone costiere, Relazione finale*. Regione Emilia-Romagna, Assessorato Ambiente e Sviluppo Sostenibile - Assessorato Sicurezza Territoriale, Difesa del Suolo e della Costa, Protezione Civile and ARPAE Emilia-Romagna, Agenzia Regionale Protezione Ambiente Energia, Bologna, Italy, 91 pp.
- Regione Emilia-Romagna and ARPAE; 2018: *Rilievo della subsidenza nella pianura emiliano romagnola, Fase II, Relazione Finale*. Regione Emilia-Romagna, Assessorato Difesa del Suolo e Della costa, Protezione Civile e Politiche Ambientali e della Montagna and ARPAE Emilia-Romagna, Agenzia Regionale Protezione Ambientale Energia, Bologna, Italy, 105 pp.
- Ricci Lucchi F., Colalongo M., Cremonini G., Gasperi G., Iaccarino S., Papani G., Raffi I. and Rio D.; 1982: *Evoluzione sedimentaria e paleogeografica del margine appenninico*. In: Cremonini G. and Ricci Lucchi F. (eds), Guida alla geologia del margine appenninico-padano, Guide Geologiche Regionali, Soc. Geol. Ital., pp. 17-46.
- Robertson P.K.; 2009: *Interpretation of Cone penetration tests - a unified approach*. Canad. Geotech. J., 46, 1337-1355.
- Robertson P.K. and Cabal K.L.; 2014: *Guide to Cone penetration testing for geotechnical engineering, 6th ed*. Gregg Drilling & Testing Inc., Signal Hill, CA, USA, 133 pp.
- Rosen P.A., Hensley S., Joughin I.R., Li F.K., Madsen S.N., Rodriguez E. and Goldstein R.; 2000: *Synthetic aperture radar interferometry*. IEEE Proc., 88, 333-382.
- Scardia G., De Franco R., Muttoni G., Rogledi S., Caielli G., Carcano C., Sciunnach D. and Piccin A.; 2012: *Stratigraphic evidence of a Middle Pleistocene climate-driven flexural uplift in the Alps*. Tectonics, 31, TC6004, doi: 10.1029/2012TC003108.
- Schlumberger Ltd; 2016: *Petrel: the platform for E&P decision making*. <www.software.slb.com>.
- Severi P.; 2021: *Soil uplift in the Emilia-Romagna plain (Italy) by satellite radar interferometry*. Boll. Geof. Teor. Appl., 62, doi: 10.4430/bgta0349, in print.
- Severi P., Mazzoni R. and Martelli L.; 2021: *Oil and gas activities in Emilia-Romagna Region (Italy): land deformation and territory protection*. Boll. Geof. Teor. Appl., 62, 269-278, doi: 10.4430/bgta0327.
- Teatini P., Gambolati G., Tomasi L. and Putti M.; 1998: *Nonlinear simulation of land subsidence over the Angela-Angelina gas field at Ravenna, Italy*. IGEA, 11, 41-48.
- Teatini P., Ferronato M., Gambolati G., Bertoni W. and Gonella M.; 2005: *A century of land subsidence in Ravenna, Italy*. Environ. Geol., 47, 831-846.
- Teatini P., Ferronato M. and Gambolati G.; 2006: *Groundwater pumping and land subsidence in the Emilia-Romagna coastland, Italy: modeling the past occurrence and the future trend*. Water Resour. Res., 42, W01406, doi: 10.1029/2005wr004242.
- Vittori E. and Ventura G.; 1995: *Grain size of fluvial deposits and late Quaternary climate: a case study in the Po River valley (Italy)*. Geol., 23, 735-738.
- Voronoi M.; 1908: *Nouvelles applications des parametres continus a la Theorie des Formes Quadratiques*. J. Reine Angewandte Math., 134, 198-287, doi: 10.1515/crll.1908.133.97.
- Zebker H.A. and Villasenor J.; 1992: *Decorrelation in interferometric radar echoes*. IEEE Trans. Geosci. Remote Sens., 30, 950-959.

Corresponding author: Ilaria Antoncecchi  
Ministero dello Sviluppo Economico, Direzione Generale per le Infrastrutture e la Sicurezza dei Sistemi Energetici e Geominerari (ex-DGS-UNMIG)  
Via A. Bosio 13b, Roma, Italy  
Phone: +39 06 470522038; e-mail: ilaria.antoncecchi.ext@mise.gov.it